

Metal Complexes with Azomethines Containing the Isomeric *E*–*Z* Azo Fragments

A. D. Garnovskii^{a,*}, A. S. Burlov^a, A. G. Starikov^b, A. V. Metelitsa^a, I. S. Vasil'chenko^a, S. O. Bezugliy^b, S. A. Nikolaevskii^a, I. G. Borodkina^a, and V. I. Minkin^{a,b}

^a Research Institute of Physical and Organic Chemistry, Southern Federal University, Rostov-on-Don, Russia

^b Southern Scientific Center, Russian Academy of Sciences, Rostov-on-Don, Russia

*E-mail: garn@ipoc.rsu.ru

Received December 1, 2009

Abstract—Cobalt and zinc complexes with phenylazosalicylaldehyde azomethines were obtained by chemical and electrochemical syntheses. The B3LYP/6-311G(*d, p*) calculations showed that the azo group in both the ligands and the complexes are mainly in the *E*-form.

DOI: 10.1134/S1070328410070018

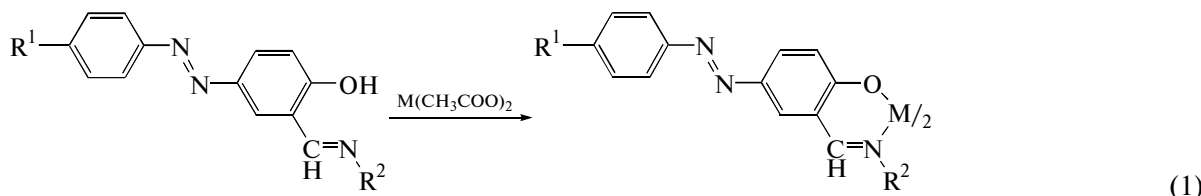
Along with various photophysical effects that change the magnetic properties of materials (selective photoinduced growth of magnetic domains, excitation of electrons resulting in crystal magnetization, radiation-induced formation of paramagnetic centers in crystals, etc.) [1, 2], photochemical transformations that enable reversible modulation of the magnetism of solids and solutions are of great interest for the preparation of a new generation of energy-independent capacious magnetic storage devices [3–5]. Among the most important mechanisms behind photoinduced transformations that lead to reversible change in the magnetism on the molecular level (spin crossover), light-induced ones include a capture of photoexcited states (LIESST) [1, 6], modifications of the crystal lattice of the anionic fragment of paramagnetic complexes of ionic photochromes [7], and a spin crossover induced by isomerization of the photochromic ligands in *d*⁴–*d*⁷ metal complexes (LD LISC) [8].

Photoinduced ligand isomerization that changes the character of the environment of the metal ion and causes the transition into the state of a different multi-

plicity has been studied mainly for isomerization of complexes with stilbene [8, 9] and azobenzene ligands [4]. Since LD LISC-type reactions accompanied by a spin crossover can occur in solutions, the study of their mechanism seems to be especially promising. We examined cobalt complexes with salicylaldimine ligands containing the photochromic azobenzene fragment.

Despite permanent interest in metal complexes with various azo ligands [10–19], the literature data on metal complexes with the N=N group being outside the coordination unit are scarce. Typical examples of the latter include complexes with azomethines containing the phenylazo group in the aldehyde fragment of chelated Schiff's bases [20–24].

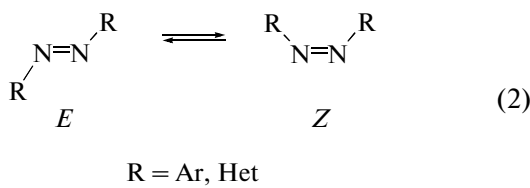
The goal of this study was to obtain metal complexes with azo ligands, perform quantum-chemical calculations, and examine the absorption and emission spectra of azo azomethine ligands (**I**) and their metal complexes (**II**) promising for the study of the crossover effect.



I: R¹ = H, R² = Ph (a);
R¹ = H, R² = (CH₂)₁₇CH₃ (b);
R¹ = C₂H₅O, R² = (CH₂)₁₁CH₃ (c);
R¹ = C₂H₅O, R² = (CH₂)₁₇CH₃ (d).

II: M = Co, R¹ = H, R² = Ph (a);
M = Zn, R¹ = C₂H₅O, R² = (CH₂)₁₇CH₃ (b);
M = Co, R¹ = C₂H₅O, R² = (CH₂)₁₁CH₃ (c);
M = Zn, R¹ = C₂H₅O, R² = (CH₂)₁₁CH₃ (d);
M = Co, R¹ = C₂H₅O, R² = (CH₂)₁₇CH₃ (e).

Special interest in ligands **I** and their complexes **II** is due to the presence of the *E*–*Z* photo- and thermo-isomerizable azo group in their molecules [25–28]:



EXPERIMENTAL

5-Phenylazosalicylaldehyde and 5-(4-ethoxyphenylazo)salicylaldehyde were prepared as described in [24].

Synthesis of azomethines **Ia–**Id**.** A solution of an appropriate amine (aniline, dodecylamine, and octadecylamine) (0.1 mol) in methanol (10 ml) was added to a solution of arylazosalicylaldehyde (0.1 mol) in methanol (10 ml). The reaction mixture was refluxed on a water bath for 1 h. On cooling, the precipitates of azomethines that formed were filtered off and recrystallized from acetonitrile.

5-Phenylazosalicylideneaminobenzene (Ia**).** The yield was 68%, yellow needles, $T_m = 140\text{--}141^\circ\text{C}$.

^1H NMR (δ , ppm): 7.26–8.07 (m, 13H, HC_{Ar}), 8.76 (s, 1H, $\text{HC}=\text{N}$), 13.90 (s, 1H, OH).

IR (ν , cm $^{-1}$): 3100–3400 (s, OH), 1638 (s, C=N), 1495 (w, N=N), 1289 (m, Ph–O).

For $\text{C}_{19}\text{H}_{15}\text{N}_3\text{O}$

anal. calcd. (%): C 75.73; H 5.02; N 13.94.
Found (%): C 75.84; H 5.12; N 14.02.

1-(5-Phenylazosalicylidene)aminoctadecane (Ib**):** yellow crystals, 60% yield, $T_m = 60\text{--}61^\circ\text{C}$.

^1H NMR (δ , ppm): 0.88 (t, 3H, CH_3 , $^3J = 6.6$ Hz), 1.18–1.36 (m, 30H, 15 CH_2), 1.73 (quintet, 2H, CH_2 , $^3J = 7.4$ Hz), 3.64 (t, 2H, CH_2 , $^3J = 6.6$ Hz), 7.04 (d, 8H, HC_{Ar} , $^3J = 9.0$ Hz), 7.43–7.53 (m, 3H, HC_{Ar}), 7.99 (dd, 1H, HC_{Ar} , $^3J = 9.0$ Hz, $^4J = 2.4$ Hz), 8.40 (s, 1H, $\text{HC}=\text{N}$), 14.46 (s, 1H, OH).

IR (ν , cm $^{-1}$): 3100–3400 (s, OH), 1636 (vs, C=N), 1494 (m, NN), 1287 (m, Ph–O).

For $\text{C}_{31}\text{H}_{47}\text{N}_3\text{O}$

anal. calcd. (%): C 77.94; H 9.92; N 8.80.
Found (%): C 77.98; H 9.84; N 8.78.

1-(5-(4-Ethoxyphenylazo)salicylidene)aminododecane (Ic**):** The yield was 75%, yellow crystals, $T_m = 69\text{--}70^\circ\text{C}$.

^1H NMR (δ , ppm): 0.85 (t, 3H, CH_3 , $^3J = 6.7$ Hz), 1.19–1.22 (m, 18H, 9 CH_2), 1.46 (t, 3H, CH_3 , $^3J = 7.0$ Hz),

1.63 (m, 2H, CH_2), 3.62 (t, 2H, CH_2 , $^3J = 7.0$ Hz), 4.11 (quintet, 2H, CH_2 , $^3J = 6.9$ Hz), 6.90–6.98 (m, 3H, HC_{Ar}), 7.79–7.98 (m, 4H, HC_{Ar}), 8.37 (s, 1H, $\text{HC}=\text{N}$), 14.35 (br.s, 1H, OH).

IR (ν , cm $^{-1}$): 3100–3400 (s, OH), 1636 (vs, C=N), 1500 (m, N=N), 1285 (m, Ph–O).

For $\text{C}_{27}\text{H}_{39}\text{N}_3\text{O}_2$

anal. calcd. (%): C 74.10; H 8.98; N 9.60.
Found (%): C 74.18; H 9.76; N 9.58.

1-[5-(4-Ethoxyphenylazo)salicylidene]aminoctadecane (Id**):** The yield was 80%, yellow crystals, $T_m = 79\text{--}80^\circ\text{C}$.

^1H NMR (δ , ppm): 0.88 (t, 3H, CH_3 , $^3J = 6.7$ Hz), 1.25–1.57 (m, 34H, 17 CH_2), 3.63 (t, 3H, CH_3 , $^3J = 7.0$ Hz), 4.11 (quintet, 2H, CH_2 , $^3J = 7.0$ Hz), 6.97–7.94 (m, 7H, HC_{Ar}), 8.39 (s, 1H, $\text{HC}=\text{N}$), 14.37 (br.s, 1H, OH).

IR (ν , cm $^{-1}$): 3100–3400 (s, OH), 1636 (vs, C=N), 1500 (m, N=N), 1285 (m, Ph–O).

For $\text{C}_{33}\text{H}_{51}\text{N}_3\text{O}_2$

anal. calcd. (%): C 75.96; H 9.85; N 8.05.
Found (%): C 75.87; H 9.64; N 8.16.

Chemical synthesis (CS) of complexes **IIa–**IId**** [29]. A solution of $\text{Co}(\text{CH}_3\text{COO})_2 \cdot 4\text{H}_2\text{O}$ or $\text{Zn}(\text{CH}_3\text{COO})_2 \cdot 2\text{H}_2\text{O}$ (1 mmol) in methanol (10 ml) was added to a solution of an appropriate azomethine **Ia**–**Id** (2 mmol) in methanol (10 ml). The reaction mixture was refluxed on a water bath for 1 h. The precipitates that formed were filtered off, recrystallized from $\text{MeOH}-\text{CHCl}_3$ (2 : 1), and dried in a vacuum desiccator.

Electrochemical synthesis (ES) of complexes **IIa–**IId**** was carried out according to a standard procedure by the reaction of azomethines **Ia**–**Id** with cations of the anode dissolved during electrolisis [30, 31]. Azomethines **Ia**–**Id** (2 mmol) were dissolved in acetonitrile (10 ml) and $[\text{Et}_4\text{N}]\text{ClO}_4$ (0.01 g) was added as a conductive agent. A current (40 mA, 15 V) was passed through the solution for 1 h. The precipitates of the resulting complexes were filtered off, recrystallized from $\text{MeOH}-\text{CHCl}_3$ (2 : 1), and dried in a vacuum desiccator. The melting temperatures and spectroscopic characteristics of the chemically and electrochemically obtained complexes are identical.

Bis(5-phenylazosalicylideneaminobenzolato)cobalt (IIa**):** The yield was 75%, red crystals, $T_m = 252\text{--}253^\circ\text{C}$, $\mu_{\text{eff}} = 4.31 \mu_B$ (293 K).

IR (ν , cm^{-1}): 1604 (vs, C=N), 1496 (m, N=N), 1319 (m, Ph-O).

For $\text{C}_{38}\text{H}_{28}\text{N}_6\text{O}_2\text{Co}$

anal. calcd. (%): C 69.20; H 4.28; N 12.74; Co 8.93.

Found (%): (CS) C 69.14; H 4.21; N 12.67; Co 8.84.

(ES) C 69.15; H 4.30; N 12.70; Co 8.96.

Bis[1-(5-phenylazosalicylidene)aminoctadecanato]zinc (IIb). The yield was 95%, yellow crystals, $T_m = 85-86^\circ\text{C}$.

^1H NMR (δ , ppm): 0.87 (t, 6H, 2CH_3 , $^3J = 6.7 \text{ Hz}$), 1.18–1.29 (m, 60H, 30CH_2), 1.58–1.65 (m, 4H, 2CH_2), 3.61 (t, 4H, 2CH_2 , $^3J = 7.2 \text{ Hz}$), 6.93 (s, 2H, HC_{Ar} , $^3J = 9.16 \text{ Hz}$), 7.40–7.52 (m, 6H, HC_{Ar}), 7.83–8.03 (m, 8H, HC_{Ar}), 8.34 (s, 2H, $2\text{HC}=\text{N}$).

IR (ν , cm^{-1}): 1614 (s, C=N), 1496 (m, N=N), 1326 (m, Ph-O).

For $\text{C}_{62}\text{H}_{92}\text{N}_6\text{O}_2\text{Zn}$

anal. calcd. (%): C 73.09; H 9.10; N 8.25; Zn 6.42.

Found (%): (CS) C 73.13; H 9.19; N 8.18; Zn 6.49.

(ES) C 73.05; H 9.14; N 8.20; Zn 6.50.

Bis{1-[5-(4-ethoxyphenylazo)salicylidene]aminoctadecanato}cobalt (IIc). The yield was 75%, a red-brown powder, $T_m = 130-131^\circ\text{C}$, $\mu_{\text{eff}} = 4.84 \mu_B$ (293 K).

IR (ν , cm^{-1}): 1616 (s, C=N), 1499 (m, N=N), 1320 (m, Ph-O).

For $\text{C}_{54}\text{H}_{76}\text{N}_6\text{O}_4\text{Co}$

anal. calcd. (%): C 69.58; H 8.22; N 9.02; Co 6.32.

Found (%): (CS) C 69.46; H 8.28; N 9.15; Co 6.42.

(ES) C 69.60; H 8.30; N 9.00; Co 6.38.

Bis{1-[5-(4-ethoxyphenylazo)salicylidene]aminoctadecanato}zinc (IId). The yield was 89%, yellow crystals, $T_m = 130-131^\circ\text{C}$.

^1H NMR (δ , ppm): 0.84 (t, 6H, 2CH_3 , $^3J = 6.7 \text{ Hz}$), 1.18–1.21 (m, 36H, 18CH_2), 1.46 (t, 6H, CH_3 , $^3J = 7.9 \text{ Hz}$), 1.62–1.65 (m, 4H, 2CH_2), 3.60 (t, 4H, 2CH_2 , $^3J = 7.0 \text{ Hz}$), 4.11 (quintet, 4H, 2CH_2 , $^3J = 6.9 \text{ Hz}$), 6.91–7.00 (m, 6H, HC_{Ar}), 7.78–7.99 (m, 8H, HC_{Ar}), 8.32 (s, 2H, $2\text{HC}=\text{N}$).

IR (ν , cm^{-1}): 1618 (s, C=N), 1499 (m, N=N), 1326 (s, Ph-O).

For $\text{C}_{54}\text{H}_{76}\text{N}_6\text{O}_6\text{Zn}$

anal. calcd. (%): C 69.10; H 8.16; N 8.95; Zn 6.97.

Found (%): (CS) C 69.18; H 8.13; N 8.87; Zn 6.82.

(ES) C 69.07; H 8.20; N 9.00; Zn 7.05.

Bis{1-[5-(4-ethoxyphenylazo)salicylidene]aminoctadecanato}cobalt (IIe). The yield was 63%, a red-brown powder, $T_m = 135-136^\circ\text{C}$, $\mu_{\text{eff}} = 4.86 \mu_B$ (293 K).

IR (ν , cm^{-1}): 1620 (s, C=N), 1500 (m, N=N), 1326 (m, Ph-O).

For $\text{C}_{66}\text{H}_{100}\text{N}_6\text{O}_4\text{Co}$

anal. calcd. (%): C 72.03; H 9.16; N 7.64; Co 5.35.

Found (%): (CS) C 72.15; H 9.14; N 7.74; Co 5.47.

(ES) C 72.08; H 9.10; N 7.58; Co 5.39.

Electronic absorption spectra were recorded on a Varian Carry 100 spectrophotometer; emission spectra were recorded on Shimadzu RF-5001 PC spectrofluorimeter. ^1H NMR spectra were recorded on a Varian Unity-300 instrument (300 MHz) in CDCl_3 with internal stabilization of the ^2H polar resonance line. IR spectra of powdery complexes I and II were recorded on a Varian 3100-FTIR Excalibur instrument by frustrated total internal reflection. The magnetic moments of solid samples were determined by the Faraday method at room temperature.

Calculations were performed by the DFT method (B3LYP/6-311++G(d, p)) using the Gaussian03 program [32]. As demonstrated in [33–35], these functional and basis set reproduce well the energy characteristics of intramolecular rearrangements in transition metal complexes. To find stationary points on the potential energy surface (PES), we fully optimized the molecular geometries and calculated the force constants. The structures that refer to the energy minima on the PES were found by a minimum energy path proceeding along the gradient line from the saddle point to its adjacent stationary (saddle or minimum) point [36]. The graphical images of the molecular structures (Figs. 1, 2) were plotted with the ChemCraft program; the Cartesian coordinates of the atoms from the quantum-chemical calculations were used as input parameters for this program.

RESULTS AND DISCUSSION

Elemental analysis (C, H, N, and M) and IR, ^1H NMR, and electronic absorption spectroscopy of azomethines I and their metal chelates II revealed that azo azomethines I exist as iminophenol tautomers in both solution and the solid state and that their reactions with Co(II) and Zn(II) acetates give the complexes ML_2 (where HL are ligands I).

When performing quantum-chemical calculations, we considered not only the relative stabilities of the E-Z tautomers (2) of free and coordinated Schiff's bases containing the phenylazo substituent but also the possibility of a square-tetrahedron equilibrium for salicylideneamine [30, 31].

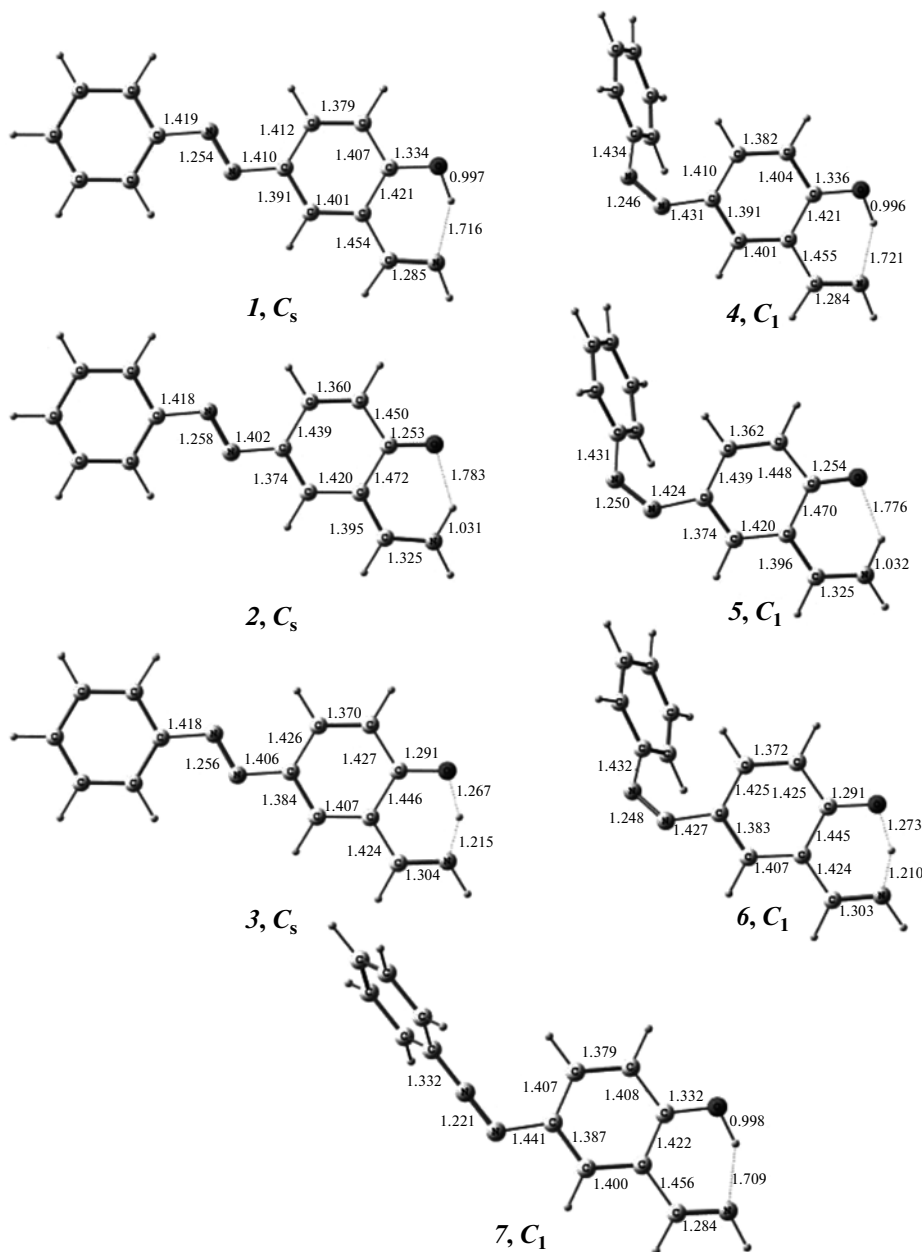


Fig. 1. DFT-calculated (B3LYP/6-311++G(*d, p*)) geometrical parameters of structures *1*–*7* (the bond lengths are cited in angstroms, also in Figs. 2 and 3).

Initially, we studied the structures and relative stabilities of different forms of the ligands ($R = H$). Our calculations showed that structure *1*, in which the azo group has the *E* configuration and the proton of the chelate ring is localized on the O atom, is characterized by the lowest total energy and, accordingly, is a global minimum (Fig. 1, Table 1).

At the same time, tautomer *2* is less stable than the iminophenol form *1* by less than 2 kcal/mol. The calculated barrier to the interconversion between these structures, which occurs by intramolecular proton transfer through transition state *3*, is 2.3 kcal/mol

(with consideration to the zero-point energy of harmonic vibrations). Therefore, structures *1* and *2* are in dynamic equilibrium with each other. The most stable *Z* conformation of the ligand (structure *4*) is thermodynamically less favorable than structure *1* by 16.3 kcal/mol. Apparently, *Z* structures *4* and *5* are also in equilibrium because of a small (2.7 kcal/mol) barrier to their prototropic isomerization involving transition structure *6*.

Although *E*–*Z* isomerization of the azo group of this ligand is induced by photoirradiation only, it was interesting to estimate the barrier to this rearrange-

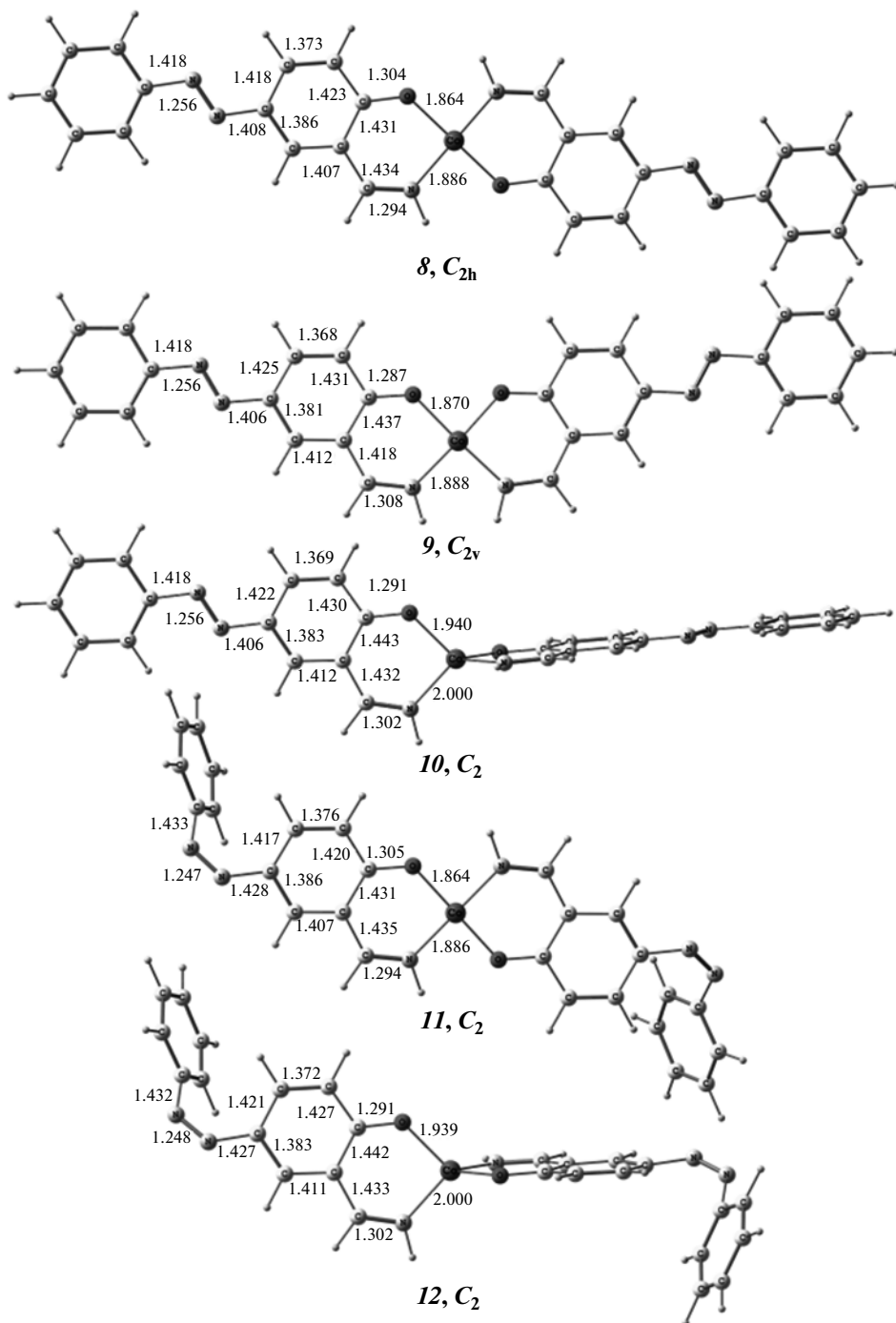


Fig. 2. DFT-calculated (B3LYP/6-311++G(*d, p*)) geometrical parameters of structures 8–12.

ment under thermal conditions. Theoretical isomerization of azobenzene has been discussed in [37–39]. DFT B3LYP calculations showed that the isomerization on the ground-state PES is prevented until a barrier of 40 kcal/mol is surmounted. An analysis of this isomerization by the CASSCF method on a triplet-excited PES revealed that the spin-forbidden transi-

tion path allows an activation energy decrease to 28 kcal/mol.

The calculated barrier to the isomerization of structure 1 proceeding through transition state 7 is 38.5 kcal/mol. This agrees well with the aforementioned calculations and suggests that the reaction is impossible under thermal conditions. Therefore, the

Table 1. Total energy E_{tot} , the relative energy ΔE , the total energy $E_{\text{tot}, \text{ZPE}}^*$ corrected to the zero-point energy of harmonic vibrations, and the relative energy ΔE_{ZPE} corrected to the zero-point energy of harmonic vibrations in structures 1–7 calculated by the DFT method (B3LYP/6-311++G(d, p)); λ is the number of imaginary Hessian eigenvalues

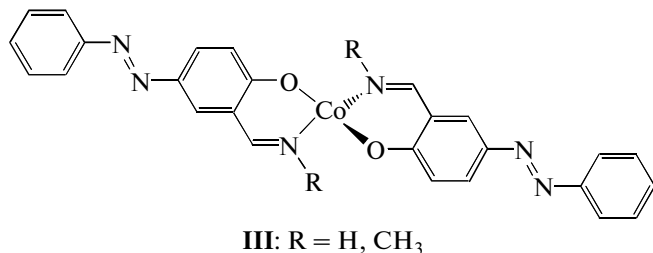
Structure, symmetry	E_{tot} , au	ΔE , kcal/mol	$E_{\text{tot}, \text{ZPE}}$, au	ΔE_{ZPE} , kcal/mol	λ
1, C_s	−741.64541	0.0	−741.42901	0	0
2, C_s	−741.64240	1.9	−741.42630	1.7	0
3, C_s	−741.63748	5.0	−741.42526	2.3	1
4, C_1	−741.61921	16.4	−741.40298	16.3	0
5, C_1	−741.61538	18.8	−741.39950	18.5	0
6, C_1	−741.61071	21.8	−741.39879	19.0	1
7, C_1	−741.58180	39.9	−741.36761	38.5	1

* ZPE is the zero-point energy of harmonic vibrations.

substituents in azobenzene have only a slight effect on the barrier to its isomerization. An analysis of the geometrical parameters of structure 7 showed that the N=N bond length in the azo group is shortened to 1.22 Å and the C=N bond length in the phenylazo group is shortened to 1.33 Å. Apparently, these changes are responsible for such a high barrier to the isomerization.

It is known that cobalt complexes with β -aminovinyl ketonates ($R = H$) in noncoordinating solvents undergo rapid isomerization associated with the transitions between the low-spin planar and high-spin

pseudotetrahedral forms. The existence of “square–tetrahedron” equilibrium in such cobalt complexes was first reported in 1966 [40, 41]. The Gibbs energy difference between the configurational isomers determined from NMR spectra depends on the substituents at the C atoms and does not exceed 3 kcal/mol. It was interesting to consider the possibility of a similar spin-crossover isomerization of the complexes under study and estimate the influence of the *E*–*Z* isomerization of the azo group on this process. For this purpose, we performed a quantum-chemical study of the stabilities of different complex forms for model structures III:



According to calculations of bischelate complexes III ($R = H$), structure 8 on a doublet-excited PES is characterized by the lowest energy and corresponds to a low-spin planar *trans*-configuration (Fig. 2). *cis*-Isomer 9 has also a minimum energy but is less stable than structure 8 by more than 10 kcal/mol. Consideration of the high-spin complex led to structure 10 corre-

sponding to the minimum on a quartet PES. In structure 10, the coordination polyhedron is a pseudotetrahedron. A small energy difference between structures 8 and 10 (0.9 kcal/mol) suggests a dynamic equilibrium between them in noncoordinating solvents.

A theoretical study of complexes with the *Z* conformation of the azo group showed that the energy differ-

Table 2. Total energy E_{tot} , the relative energy ΔE , the total energy $E_{\text{tot}, \text{ZPE}}$ corrected to the zero-point energy of harmonic vibrations, and the relative energy ΔE_{ZPE} corrected to the zero-point energy of harmonic vibrations in structures 8–16 calculated by the DFT method (B3LYP/6-311++G(d, p))

Structure, symmetry	Multiplicity	E_{tot} , au	ΔE , kcal/mol	$E_{\text{tot}, \text{ZPE}}$, au	ΔE_{ZPE} , kcal/mol
$R = H$					
8, C_{2h}	2	−2864.96081		−2864.54582	
9, C_{2v}	2	−2864.94559	9.6	−2864.52905	10.5
10, C_2	4	−2864.95741	2.1	−2864.54445	0.9
11, C_2	2	−2864.90778	33.3	−2864.49332	32.9
12, C_2	4	−2864.90416	35.5	−2864.49172	33.9
$R = CH_3$					
13, C_2	4	−2943.59296		−2943.12549	
14, C_{2h}	2	−2943.58618	4.3	−2943.11613	5.9
15, C_2	4	−2943.53986	33.3	−2943.07292	33.0
16, C_2	2	−2943.53326	37.5	−2943.06368	38.8

ence between low-spin planar structure 11 and high-spin structure 12 is of the same order of magnitude as that between the aforesaid *trans*-isomers 8 and 10. Therefore, they can also exist in equilibrium with each other. We calculated that the complex with the *E*-azo group is more stable by ~33 kcal/mol than the complex with the *Z*-azo group (Table 2); this value equals the double energy difference between the different forms of the ligands. Such a considerable energy difference between the structures with the *Z*- and *E*-azo groups precludes thermal equilibrium in solutions of complexes III.

Replacement of the substituent at the N atom (III: $R = Me$) stabilizes the high-spin pseudotetrahedral configuration of the complex (structure 13, Fig. 3), while low-spin planar structure 14 is less stable by 5.9 kcal/mol. Similar results were obtained for the complex with the *Z*-azo group. The calculated energy difference between structures 15 and 16 (5.8 kcal/mol) provides evidence for a high-spin form.

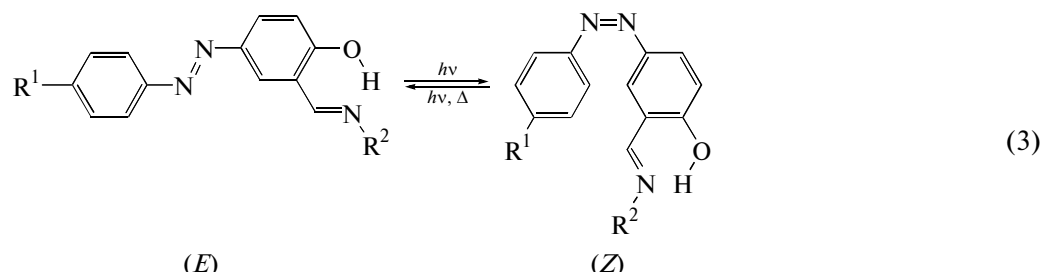
Thus, one can conclude that the *E*–*Z* isomerization of the azo group in complexes III does not influence the relative stabilities of their high- and low-spin

forms, regardless of the substituents in the chelate ring and the spin state. At the same time, replacement of the functional groups at the donor N atom ($R = H$ by $R = CH_3$) changes the ground-state multiplicity in the Co(II) bischelates studied.

The electronic absorption spectra of the most stable *E*-isomers of azobenzenes I (3) containing the azomethine fragment in DMF show unsymmetrical absorption bands at 336–369 nm (ϵ 23560–34290 1 mol^{−1} cm^{−1}) and less intense bands as a shoulder at 430–455 nm (ϵ 5120–9270 1 mol^{−1} cm^{−1}) (Table 3, Fig. 4).

The intense absorption bands belong to the $\pi\pi^*$ -type and the less intense longer-wavelength bands belong to the $n\pi^*$ -type [42]. Introduction of the azomethine fragment mainly shifts the $\pi\pi$ -type band to the longer wavelengths compared to its position for unsubstituted azobenzene, which results in partial overlap of the $\pi\pi^*$ - and $n\pi^*$ -type bands (Fig. 4).

Like most of the earlier examined azobenzenes, the *Z*-isomers of compounds I do not fluoresce [43].



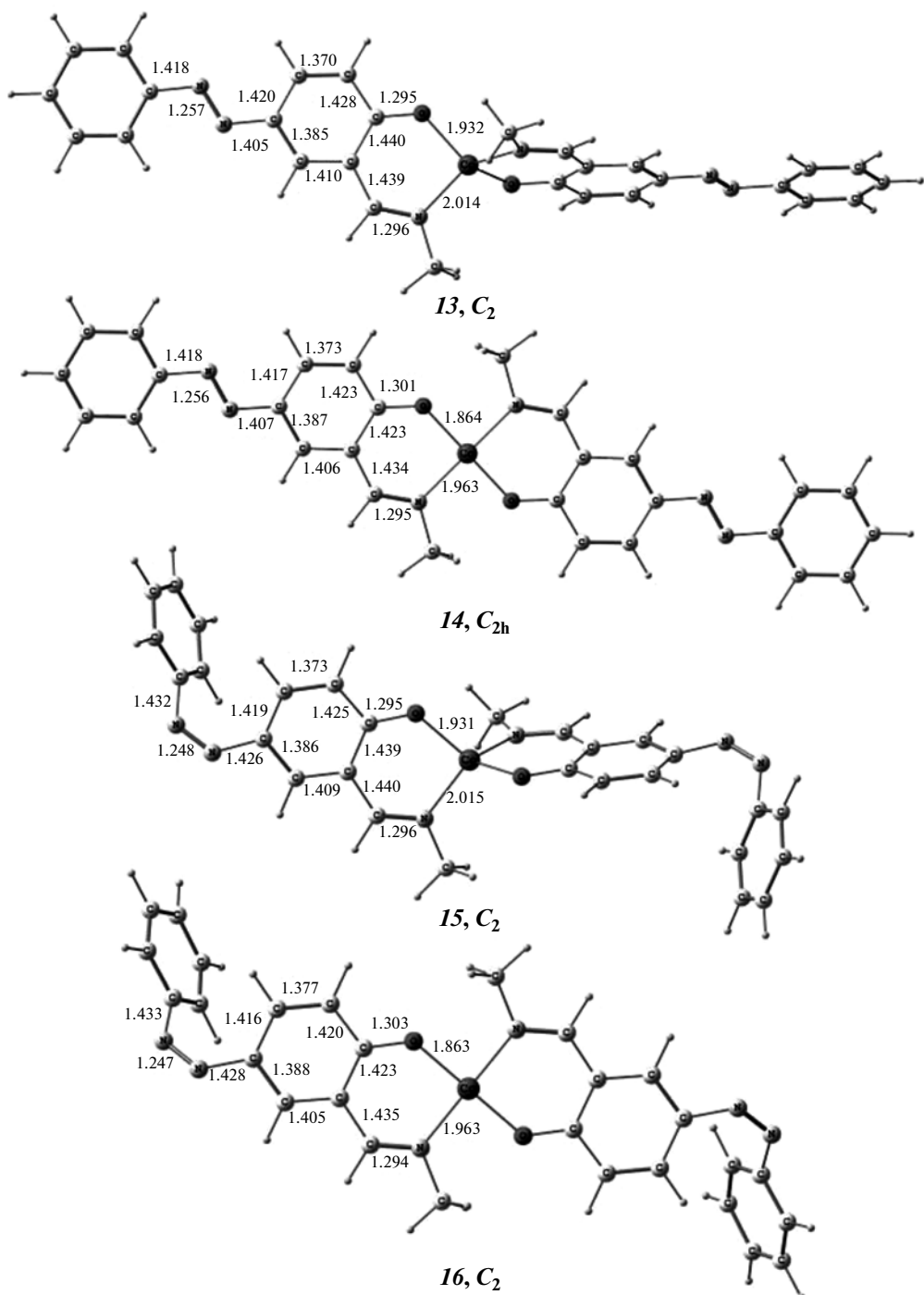


Fig. 3. DFT-calculated (B3LYP/6-311++G(*d, p*)) geometrical parameters of structures *13–16*.

Irradiation of solutions of compounds **I** at the wavelengths of both the $\pi\pi^*$ - and $n\pi^*$ -type bands induced *E*–*Z* isomerization characteristic of azobenzenes, which made the longer-wavelength bands less intense and caused a bathochromic shift of the $\pi\pi^*$ -type bands and a slight hypsochromic shift of the $n\pi^*$ -type bands [44] (Table 3, Fig. 5).

After the irradiation was stopped, the absorption spectra of compounds **I** returned to their original shapes because of thermal *E*–*Z* isomerization. The *Z*-isomers of substituted azobenzenes **I** are substantially less stable than the *Z*-isomer of unsubstituted derivative (Table 3). The characteristic relaxation times in N-alkyl derivatives **1b–1d** is more than one order of magnitude than those in N-phenyl azoben-

Table 3. Spectral absorption and kinetic characteristics of azobenzenes **I** and their metal complexes **II** in DMF at 293 K

Compound	Initial form, <i>E</i>		Photostationary state	Characteristic times of the thermal relaxation processes
	λ_{\max} , nm	ε_{\max} , l mol ⁻¹ cm ⁻¹	λ_{\max} , nm	$\tau_{293}(Z)$, s*
Ia	336	30890	332	0.1
	455 sh	5120		
Ib	363	23560	350	1.1
	430 sh	8660		
Ic	369	29970	363	1.6
	440 sh	8070		
Id	369	34290	363	1.7
	440 sh	9270		
Azobenzene	317	17000	302	1.6×10^5 [40]**
	438	500		
IIa	398	60770	396	128
	449 sh	44560		
IIb	381	66790	367	0.8
	431 sh	31710		9.7
IIc	399	61620	385	23
	445 sh	46570		214
IId	380	64280	365	0.6
	430	30510		8.4
IIe	393	53180	375	23 480

Notes: * The lifetime of the *Z*-form.

** Benzene, 308 K.

zene **Ia**. The *E*–*Z* isomerization, along with its rapid thermal reverse, prevents complete photoinduced conversion of the *E*-isomers into the *Z*-forms because of considerable overlap of their absorption bands. Irradiation leads to a photostationary state in which the ratio of the isomers depends on the wavelength and intensity of the exciting light.

The electronic absorption spectra of Co (**IIa**, **IIc**, and **IIe**) and Zn complexes (**IIb** and **IId**) with azomethine ligands containing a photochromic azobenzene fragment show longer-wavelength peaks at 381–399 nm (Table 3, Fig. 4). These bands are unsymmetrical, having a shoulder at 431–449 nm. The influence of the metal nature manifests itself in the longer-wavelength range for the cobalt complexes compared to the zinc ones. Neither cobalt nor zinc complexes were found to fluoresce.

Irradiation of complexes **II** at the wavelengths of their longer-wavelength absorption bands induced photochromic transformations resulting in the decreasing intensities and hypsochromic shifts of the peaks (Figs. 6, 7). The established photostationary state for the zinc complexes is more strongly shifted toward the photoproducts than for the cobalt complexes. The kinetics of the relaxation processes in the

complexes is generally biexponential; the characteristic times of the thermal reactions for the cobalt complexes are longer than the corresponding values for the zinc complexes (Table 3). It can be seen from the presented data that both the time constants of the photo-induced relaxation processes in the complexes are one to two orders of magnitude higher than the time constant of the thermal *E*–*Z* isomerization in the ligands. The photostationary states in the ligands and the complexes are appreciably different: the absorption spectra of the complexes differ only slightly prior to irradiation and after establishing the photostationary state, while spectral changes in the ligands are substantial. Therefore, a reverse photoreaction can bring the molecular system to the initial state, the reverse photoreactions being more efficient for the cobalt complexes (cf. Figs. 6, 7).

To find out whether complexes **II** can exhibit a ligand-induced crossover effect, low-temperature magnetochemical studies (with and without UV irradiation) of Co(II) and Fe(II, III) complexes are required.

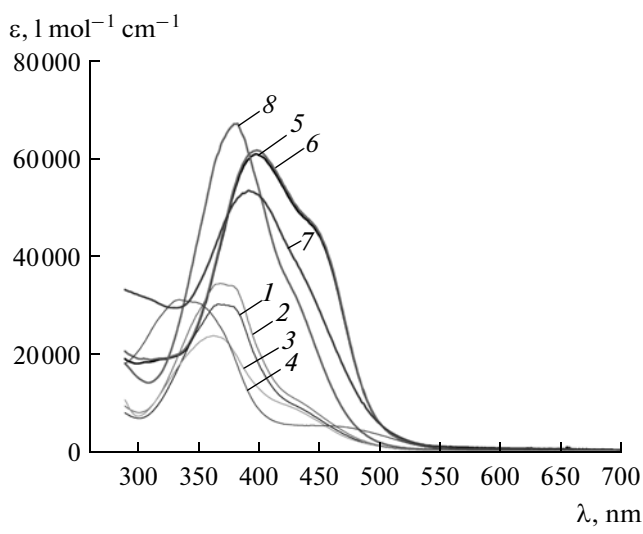


Fig. 4. Electronic absorption spectra of arylazosalicylaldimines (1) **Ic**, (2) **Id**, (3) **Ib**, and (4) **Ia** and their metal complexes (5) **IIa**, (6) **IIc**, (7) **IIe**, and (8) **IIb** in DMF at 293 K.

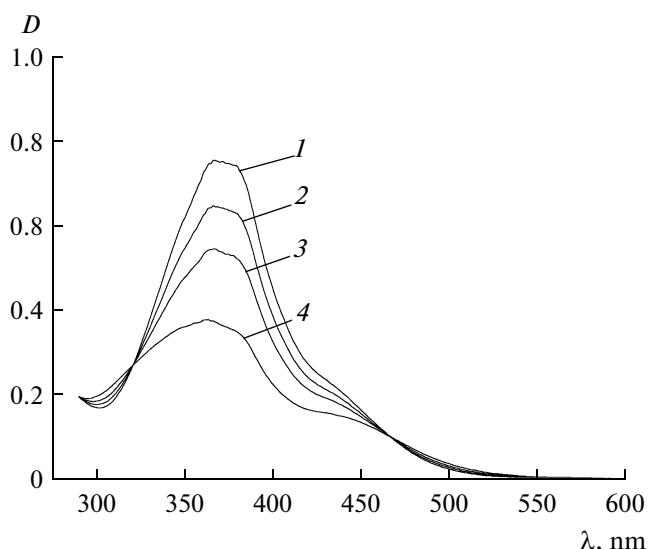


Fig. 5. Electronic absorption spectra of azobenzene **Id** in DMF (1) prior to and after the irradiation with UV light ($\lambda = 365 \text{ nm}$) for (2) 20, (3) 40, and (4) 70 s ($c = 2.51 \times 10^{-5} \text{ mol/l}$, 293 K).

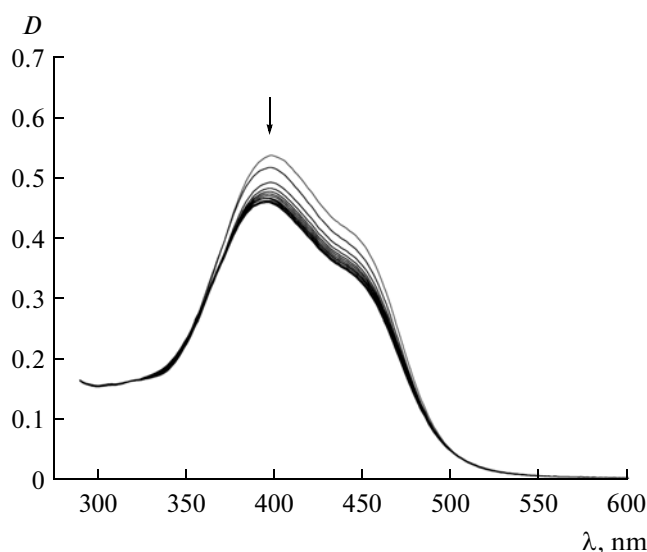


Fig. 6. Electronic absorption spectra of cobalt complex **IIc** irradiated with UV light ($\lambda = 365 \text{ nm}$) in DMF at 293 K ($c = 8.90 \times 10^{-5} \text{ mol/l}$). The spectra were recorded with 10-s intervals.

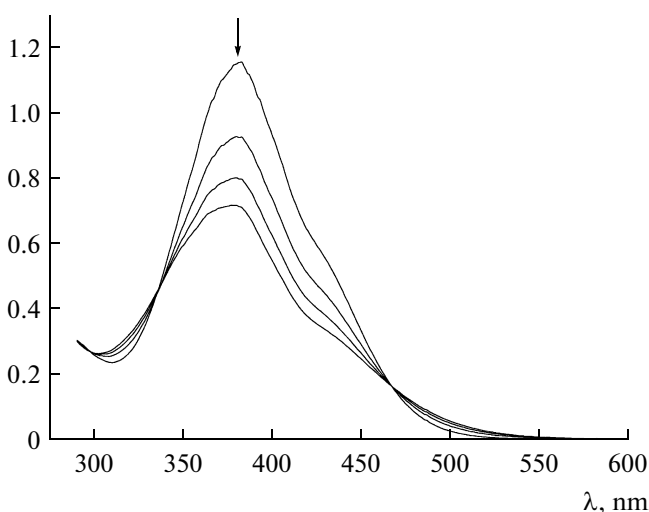


Fig. 7. Electronic absorption spectra of zinc complex **IIb** irradiated with UV light ($\lambda = 365 \text{ nm}$) in DMF ($c = 1.71 \times 10^{-5} \text{ mol/l}$, 293 K). The spectra were recorded with 2-s intervals.

ACKNOWLEDGMENTS

This work was supported by the Russian Foundation for Basic Research (project no. 09-03-12109ofi_m).

REFERENCES

- Sato, O., *J. Photochem. Photobiol., C*, 2004, vol. 5, no. 3, p. 203.
- Einaga, Y., *J. Photochem. Photobiol., C*, 2006, vol. 7, nos. 2–3, p. 69.
- Minkin, V.I., *Izv. Akad. Nauk, Ser. Khim.*, 2008, no. 4, p. 673.
- Hasegawa, Y., Kume, S., and Nishihara, H., *Dalton Trans.*, 2009, no. 2, p. 280.
- Nihei, M., Shiga, T., Naeda, Y., and Oshio, H., *Coord. Chem. Rev.*, 2007, vol. 251, nos. 21–24, p. 2606.

6. Hauser, A., *Coord. Chem. Rev.*, 1991, vol. 111, no. 1, p. 275.
7. Aldoshin, S.M., *J. Photochem. Photobiol. A*, 2008, vol. 200, no. 1, p. 19.
8. Boillov, M.-L., Zarembowitch, J., and Sour, A., *Top. Curr. Chem.*, 2004, vol. 234, p. 261.
9. Guttlich, P., Garcia, Y., and Woike, T., *Coord. Chem. Rev.*, 2001, vol. 219–221, no. 1, p. 839.
10. Kogan, V.A. and Shcherbakov, I.N., *Ross. Khim. Zh.*, 2004, vol. 49, no. 1, p. 69.
11. Burlov, A.S., Uraev, A.I., Lysenko, K.A., et al., *Koord. Khim.*, 2006, vol. 32, no. 9, p. 714 [*Russ. J. Coord. Chem.* (Engl. Transl.), vol. 32, no. 9, p. 686].
12. Burlov, A.S., Uraev, A.I., Matuev, P.V., et al., *Koord. Khim.*, 2008, vol. 34, no. 12, p. 916 [*Russ. J. Coord. Chem.* (Engl. Transl.), vol. 34, no. 12, p. 904].
13. Bhunia, P., Sardar, D., and Sarker, K.K., *J. Coord. Chem.*, 2009, vol. 62, no. 4, p. 552.
14. Taher, M.A., Jarlnabbi, S.E., Ak-Sehem, A.G.M., et al., *J. Coord. Chem.*, 2009, vol. 62, no. 8, p. 1293.
15. Byabartta, P., *Koord. Khim.*, 2009, vol. 35, no. 8, p. 592 [*Russ. J. Coord. Chem.* (Engl. Transl.), vol. 35, no. 8, p. 582].
16. Kume, S. and Nishihara, H., *Dalton Trans.*, 2008, no. 25, p. 3260.
17. Chalupa, J., Dusek, L., Pedelkova, Z., et al., *J. Coord. Chem.*, 2009, vol. 62, no. 9, p. 1525.
18. Nandi, S., Bannerjee, D., Wu, J.-S., et al., *Eur. J. Inorg. Chem.*, 2009, no. 26, p. 3972.
19. Ross, T.M., Neville, S.M., Innes, D.S., et al., *Dalton Trans.*, 2010, no. 39, p. 149.
20. Khandar, A.A. and Rezvani, Z., *Polyhedron*, 1999, vol. 18, no. 2, p. 129.
21. Cenati, F., Caruso, U., Centore, R., et al., *Inorg. Chim. Acta*, 2004, vol. 357, no. 2, p. 548.
22. Khandar, A.A., Hosseni-Yazdi, S.A., and Zarei, S.A., *Inorg. Chim. Acta*, 2005, vol. 358, no. 11, p. 3211.
23. Rezvani, Z., Chanea, M.A., Nejati, K., et al., *Polyhedron*, 2009, vol. 28, no. 14, p. 2913.
24. Burlov, A.S., Nikolaevskii, S.A., Bogomyakov, A.S., et al., *Koord. Khim.*, 2009, vol. 35, no. 7, p. 495 [*Russ. J. Coord. Chem.* (Engl. Transl.), vol. 35, no. 7, p. 486].
25. Dürr, H. and Bouas-Laurent, H., *Photochromism: Molecules and Systems*, Amsterdam: Elsevier, 1218.
26. Kawata, S. and Kawata, Y., *Chem. Rev.*, 2000, vol. 100, no. 5, p. 1777.
27. Delaire, J.A. and Nakatani, K., *Chem. Rev.*, 2000, vol. 100, no. 5, p. 1817.
28. Khandar, A.A., Nejati, K., and Rezvani, Z., *Molecules*, 2005, no. 10, p. 302.
29. *Synthetic Coordination and Organometallic Chemistry*, Garnovskii, A.D. and Kharisov, B.I., Eds., New York: Marcel Dekker, 2003.
30. *Direct Synthesis of Coordination and Organometallic Compounds*, Garnovskii, A.D. and Kharisov, B.I., Eds., Amsterdam: Elsevier, 1999.
31. Kharisov, B.I., Garnovskii, A.D., Kharissova, O.V., et al., *J. Coord. Chem.*, 2007, vol. 60, nos. 12–14, p. 1435.
32. Frisch, M.J., *Gaussian 0. Revision E.01*, Wallingford (CT): Gaussian Inc., 2004.
33. Starikov, A.G., *Ross. Khim. Zh.*, 2009, vol. 53, no. 1, p. 115.
34. Starikov, A.G., Minyaev, R.M., and Minkin, V.I., *Chem. Phys. Lett.*, 2008, vol. 459, p. 27.
35. Starikov, A.G., Minyaev, R.M., and Minkin, V.I., *J. Mol. Struct.*, 2009, vol. 895, no. 1, p. 138.
36. Minyaev, R.M., *Usp. Khim.*, 1994, vol. 63, no. 11, p. 939.
37. Cembran, A., Bernardi, F., Garavelli, M., et al., *J. Am. Chem. Soc.*, 2004, vol. 126, no. 10, p. 3234.
38. Wang, L., Xu, W., Yi, C., and Wang, X., *J. Mol. Graph. Mod.*, 2009, vol. 27, no. 7, p. 792.
39. Wang, L., Xu, J., Zhou, H., et al., *J. Photochem. Photobiol. A*, 2009, vol. 205, nos. 2–3, p. 104.
40. Everett, G.W. and Holm, R.H., *J. Am. Chem. Soc.*, 1966, vol. 88, no. 11, p. 2442.
41. Everett, G.W. and Holm, R.H., *Inorg. Chem.*, 1968, vol. 7, no. 4, p. 776.
42. Griffiths, J., *Chem. Soc. Rev.*, 1972, vol. 1, no. 4, p. 481.
43. *Photochromism*, Dürr, H. and Boues-Laurent, H., Eds., Amsterdam: Elsevier, 1990, p. 165.
44. Talaty, E.R. and Fargo, J.C., *Chem. Commun.*, 1967, no. 2, p. 65.